Paranodal junction formation and spermatogenesis require sulfoglycolipids

Koichi Honke*†‡, Yukie Hirahara†§, Jeffrey Dupree¶‖, Kinuko Suzuki¶‖, Brian Popko‖, Kikuro Fukushima, Junko Fukushima††, Takashi Nagasawa§, Nobuaki Yoshida‡‡, Yoshinao Wada§, and Naoyuki Taniguchi***

*Department of Biochemistry, Osaka University Medical School, 2-2 Yamadaoka, Suita, Osaka 565-0871, Japan; §Research Institute, Osaka Medical Center for Maternal and Child Health, 840 Murodo-cho, Izumi, Osaka 594-1101, Japan; ¶Department of Pathology and Laboratory Medicine and ‖Neuroscience Center, University of North Carolina, Chapel Hill, NC 27599; **Department of Physiology, Hokkaido University School of Medicine, Sapporo 060-8638, Japan; ††Department of Physical Therapy, College of Medical Technology, Hokkaido University, Sapporo 060-0812, Japan; and ‡‡Center for Experimental Medicine, Institute of Medical Science, Tokyo University, Tokyo 108-8639, Japan

Communicated by Sen-itiroh Hakomori, Pacific Northwest Research Institute, Seattle, WA, February 5, 2002 (received for review December 27, 2001)

Mammalian sulfoglycolipids comprise two major members, sulfatide (HSO_3-3-galactosylceramide) and seminolipid (HSO_3-3-monogalactosylalkylacylglycerol). Sulfatide is a major lipid component of the myelin sheath and serves as the epitope for the well known oligodendrocyte-marker antibody O4. Seminolipid is synthesized in spermatocytes and maintained in the subsequent germ cell stages. Both sulfoglycolipids can be synthesized *in vitro* by using the isolated cerebroside sulfotransferase. To investigate the physiological role of sulfoglycolipids and to determine whether sulfatide and seminolipid are biosynthesized *in vivo* by a single sulfotransferase, *Cst*-null mice were generated by gene targeting. *Cst*$^{-/-}$ mice lacked sulfatide in brain and seminolipid in testis, proving that a single gene copy is responsible for their biosynthesis. *Cst*$^{-/-}$ mice were born healthy, but began to display hindlimb weakness by 6 weeks of age and subsequently showed a pronounced tremor and progressive ataxia. Although compact myelin was preserved, *Cst*$^{-/-}$ mice displayed abnormalities in paranodal junctions. On the other hand, *Cst*$^{-/-}$ males were sterile because of a block in spermatogenesis before the first meiotic division, whereas females were able to breed. These data show a critical role for sulfoglycolipids in myelin function and spermatogenesis.

A considerable body of data has accumulated to date on the biological importance of sulfated glycoconjugates (1–6). Two major sulfated glycolipids exist in the mammal: the sulfatide HSO_3-3-galactosylceramide (GalCer), which is a sphingolipid, and the seminolipid HSO_3-3-monogalactosylalkylacylglycerol (GalEAG), which is a glycerolipid (7, 8). Sulfatide is a major lipid component of the myelin sheath and is synthesized in the oligodendrocytes in the central nervous system, as well as Schwann cells in the peripheral nervous system. Sulfatide serves as one of the epitopes for the well known oligodendrocyte-marker antibody O4 (9). Seminolipid is synthesized in spermatocytes and maintained in the subsequent germ cell stages (7, 8). The fact that the distribution of sulfoglycolipids is tissue-specific suggests that their biological roles are at the sites where they are expressed (7, 8). Despite the volume of findings as the result of *in vitro* experiments with exogenous sulfoglycolipids (7), definitive evidence relating to their physiological functions has not yet appeared.

The sulfate group of the sulfoglycolipids is transferred from 3′-phosphoadenosine 5′-phosphosulfate by means of catalysis by a glycolipid-specific sulfotransferase, GalCer sulfotransferase [cerebroside sulfotransferase (CST); EC 2.8.2.11], which is located in the Golgi membranes (7). CST has been purified to apparent homogeneity from human renal cancer cells (10), and its cDNA has been cloned (11). The mouse and human *CST* genes have also been cloned (12, 13). The purified CST was found to catalyze the synthesis of seminolipid and sulfatide *in vitro* (10). A Northern blot analysis of mouse tissues revealed that CST mRNA is expressed in brain, testis, kidney, stomach, small intestine, liver, and lung (12), all of which are tissues where sulfoglycolipids are expressed (7). No reports have been published on the existence of isozymes of CST. These observations suggest that the CST is completely responsible for the biosynthesis of both sulfoglycolipids *in vivo*.

Insight into the physiological function of sulfoglycolipids was provided by gene-targeted disruption of ceramide galactosyltransferase (CGT) (14, 15). This single enzyme, CGT, is responsible for the biosynthesis of GalCer and GalEAG, which are the precursors of sulfatide and seminolipid, respectively (14–16). CGT-knockout mice are completely devoid of GalCer and sulfatide in the brain (14, 15) and of GalEAG and seminolipid in the testis (16). CGT-deficient mice manifest neurological disorders caused by myelin dysfunction (14, 15) and the complete inhibition of spermatogenesis at the late-pachytene spermatocyte stage (16). These results provide strong support for the view that the intermediate products, GalCer and GalEAG, and/or the end products, sulfatide and seminolipid, are indispensable for myelin function and spermatogenesis. However, the creation of sulfotransferase-deficient mice would be highly desirable to understand completely the functions of the precursor galactolipids and their sulfated products (14–16).

To address this problem and to determine whether a single enzyme is responsible for the biosynthesis of both sulfatide and seminolipid *in vivo*, CST-deficient mice were created by means of gene targeting. CST-knockout mice demonstrated the essentiality of sulfoglycolipids in at least two physiological processes.

BIOCHEMISTRY

Materials and Methods

Gene Targeting. Overlapping λ clones encompassing *Cst* were isolated from a mouse 129SvJ genomic library and sequenced (12). A targeting vector was constructed by inserting a 1.6-kb *pgk-neo* cassette between two homologous flanking fragments of 7.7 kb (*Xba*I–*Sac*I) and 1.1 kb (*Sac*I-*Spe*I), flanked with a *phsv-tk* gene. A linearized vector (30 μg) was transfected into E14.1 embryonic stem cell line. Clones were selected with G418 and ganciclovir. An analysis of selected clones by Southern blot with 5′ and 3′ probes (Fig. 1) revealed that 10% (12 of 121) of the embryonic stem clones had undergone correct homologous recombination. Targeted cell clones were then injected into C57BL/6 blastocysts. Germ-line transmission of the mutant allele was achieved from male chimeras derived from embryonic stem clone cst no. 98 and cst no. 112.

Abbreviations: CGT, ceramide galactosyltransferase; CST, cerebroside sulfotransferase; GalEAG, monogalactosylalkylacylglycerol; GalCer, galactosylceramide; RT, reverse transcription.

†K.H. and Y.H. contributed equally to this work.

‡To whom reprint requests should be addressed. E-mail: khonke@biochem.med.osaka-u.ac.jp.

The publication costs of this article were defrayed in part by page charge payment. This article must therefore be hereby marked "*advertisement*" in accordance with 18 U.S.C. §1734 solely to indicate this fact.

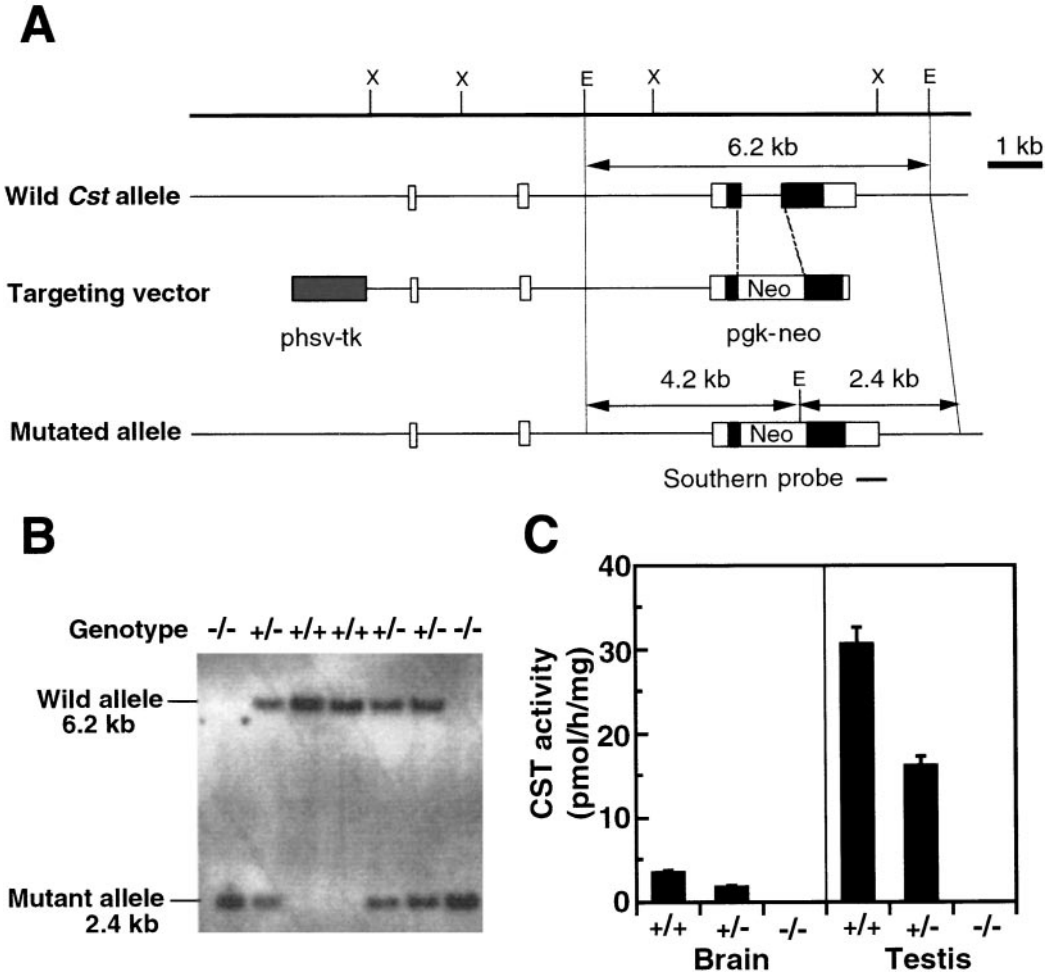

Fig. 1. Targeted disruption of the *Cst* locus and the establishment of a mutant mouse strain. (*A*) The *Cst* gene (wild allele; *Top*), the targeting vector (*Middle*), and the disrupted *Cst* locus (mutated allele; *Bottom*). Boxes represent exons. Black boxes indicate coding sequence, and open boxes denote the untranslated region sequence. This gene contains multiple exons 1, and the coding region is encoded by two exons, exons 2 and 3 (12). A 1,126-bp deletion, including 75 bp of exon 2 encoding the transmembrane domain, intron 2, and 175 bp of exon 3 encoding the 5′-3′-phosphoadenosine 5′-phosphosulfate-binding motif, was replaced with a *pgk-neo* cassette. The expected size of an *Eco*RV digestion product of the gene, hybridizing with the indicated probe, is shown for the wild allele (6.2 kb) and for the mutated allele (2.4 kb). Restriction enzyme sites: E, *Eco*RV; X, *Xba*I. (*B*) Genomic DNA isolated from F_2 littermates of the intercross of $Cst^{+/-}$ heterozygous mice was digested with *Eco*RV, blotted, and hybridized with the probe in *A*. Genotypes of the progeny are indicated at the top of each lane. (*C*) CST activity levels of brain and testis from $Cst^{+/+}$ (+/+), $Cst^{+/-}$ (+/−), and $Cst^{-/-}$ (−/−) mice. CST activity was assayed as described (10). The values represent the mean ± SE for six adult animals per group.

Animals and Tissue Processing for Light and Electron Microscopy Studies. For morphological investigations of the nervous system, $Cst^{-/-}$ mice and their littermate controls, ranging from 13 to 36 weeks in age, were anesthetized with ether and perfused with 4% paraformaldehyde alone or a solution containing 4% paraformaldehyde and 2.5% glutaraldehyde in 0.1 M sodium phosphate buffer (pH 7.4). They were immersed in the same fixative for several days. The brain, optic nerve, and spinal cord were then removed. Tissues were processed for paraffin and plastic embedding, sectioned, and examined by light microscopy as described (17). The paraffin sections were stained with solochrome and eosin, Luxol fast blue/periodic acid Schiff, and Bielschowsky stains. Plastic-embedded tissues were sectioned 1 μm thick and stained with toluidine blue. Selected areas of the plastic-embedded cerebellar tissues were thin-sectioned, double-stained with uranyl acetate and lead citrate, and examined by electron microscopy.

Testes were dissected, fixed in Bouin's solution, and embedded in paraffin. Sections (7 μm) were prepared and stained with hematoxylin/periodic acid Schiff reagent. *In situ* labeling of apoptotic cells was performed on tissue sections prepared in the same manner with an *in situ* Apoptosis Detection kit (Takara Shuzo, Kyoto), according to the manufacturer's protocol.

Electrophysiological Analysis. Peripheral and central nerve conduction velocity was measured in a total of 24 mice (5 $Cst^{-/-}$ and 19 wild-type). Each animal was initially sedated with halothane, and then anesthetized with Nembutal (0.06–0.1 mg/kg, i.p.). The sciatic nerve was exposed and single stimulating pulses (0.1-ms duration, 0.1–1 mA, at 1/s) were applied to the proximal and distal portions of the sciatic nerve, while compound electromyographic activity of the triceps surae muscle was recorded by using bipolar electrodes placed on the muscle. The latency of the direct response (i.e., M wave) was recorded. Maximal motor nerve conduction velocity was measured by dividing the latency difference recorded at the two sites by the distance between the two points. For several mice, conduction velocity was examined bilaterally. Central nerve conduction velocity was estimated in two $Cst^{-/-}$ and two wild-type mice by recording pyramidal tract volleys of the dorsal column at C1 from the spinal cord surface

in response to stimulation of the sensorimotor cortex by using bipolar electrodes, which were positioned on the pial surface. Single stimulating pulses (0.1-ms duration, 1–5 mA) were applied at 10 Hz. The direct (not synaptic) response was confirmed as fixed latency during high-frequency stimulation. Because no sensory fibers project directly to the sensorimotor cortex, a direct response must be the result of pyramidal tract activation. Only the latency of the direct response was measured and compared between the two groups. That response is a reflection of fastest pyramidal tract fibers. All experiments were performed in strict compliance with the *Guide for the Care and Use of Laboratory Animals* (18). Specific protocols were approved by the Animal Care and Use Committee of Hokkaido University School of Medicine (protocol no. 11090).

Lipid Extraction and Separation of Acidic Glycolipids. Total lipid was extracted from brain and testis with chloroform/methanol/water (30:60:8 by volume) followed by chloroform/methanol (2:1 by volume). The extracts were combined and applied to a DEAE-Sephadex A-25 (Amersham Pharmacia) column. After washing with chloroform/methanol/water (30:60:8 by volume) and methanol, acidic glycolipids were eluted with 200 mM ammonium acetate in methanol and desalted with a SepPak C18 cartridge (Waters).

Northern Blot Analysis. Total brain RNA (20 μg) was denatured in 50% (vol/vol) formamide, 6% (vol/vol) formaldehyde, 20 mM Mops (pH 7.0) at 65°C, electrophoresed in 1% agarose gel containing 6% formaldehyde, transferred to a nylon membrane (Roche Diagnostics), and hybridized with a digoxigenin-labeled (−) strand RNA probe as described (12). To generate RNA probes, cDNA fragments of *Cgt* (accession no. L21698), *Mag* (M31811), *Mbp* (M15060), and *Plp* (M15442) were obtained by reverse transcription (RT)–PCR and subcloned into pGEM-T vector (Promega).

RT-PCR Analysis. Total testicular RNA (2 μg) was reverse-transcribed with an oligo(dT) primer. The resulting cDNA was amplified by PCR by using the following primer sets: *Hlf3* (accession no. X72805), 5′-TCTTGACCATGTCGGAAACG-3′ and 5′-CTTTGGCGGGGCTTTTACGT-3′; *Sprm-1* (L23864), 5′-CTATGTTTGGGAAGGTTCTC-3′ and 5′-CCTCACTAAGTCAGAGAACT-3′; *Ccna1* (X84311), 5′-GCTGTGGCTTACTAGGCAAT-3′ and 5′-GCTGCTTCCTCATGTAGTGA-3′; *Cdc25c* (U15562), 5′-GTTAACTGGCAAGGATTTTC-3′ and 5′-GAATTCACAGAGGAACACAA-3′; *Prm1* (K02926), 5′-TCACAGGTTGGCTGGCTCGA-3′ and 5′-ATTGGCAGGTGGCATTGTTC-3′; *βactin* (X03672), 5′-TTACCAACTGGGACGACATG-3′ and 5′-AGGAGCCAGAGCAGTAATCT-3′.

Results and Discussion

A targeted disruption of *Cst* was generated through homologous recombination in embryonic stem cells. The targeting construct was designed to replace the exon portions which encode for the transmembrane domain and the 5′-3′-phosphoadenosine 5′-phosphosulfate-binding motif (19) with a neomycin-resistance cassette (Fig. 1*A*). Genotypes of pups from intercrosses between heterozygous mice were determined by Southern blotting (Fig. 1*B*). $Cst^{-/-}$ mice were born with approximately the expected Mendelian inheritance, indicating that CST is not critical for embryonic development. Northern blot analysis of brain RNA (Fig. 2*C*) and RT-PCR analysis of testicular RNA (Fig. 3*E*) showed that expression of full-length *Cst* mRNA was abolished in homozygous mice. Moreover, CST activity levels in brain and testis were correlated with its gene dosage (Fig. 1*C*), indicating that no other isozyme is expressed in these tissues.

$Cst^{-/-}$ mice were born healthy, but began to display hindlimb weakness by 6 weeks of age (Fig. 2*A*). These mutant mice subsequently showed a pronounced tremor and progressive ataxia. Involuntary movement also appeared in some $Cst^{-/-}$ mice. The *Cst*-null mice, however, are able to survive to more than 1 year of age. The phenotype of the CST-deficient mice was milder than that of CGT-deficient mice in terms of the age of onset, life span, and the severity of symptoms (14, 15). $Cst^{-/-}$ mice showed a complete loss of sulfatide in brain (Fig. 2*B*), proving that only one *Cst* gene is responsible for the biosynthesis of sulfatide in the myelin sheath. No changes in other glycolipid composition, including GalCer (Fig. 2*B*), were detected, suggesting that loss of sulfatide is the primary cause of the neurological disorder. No differences in the level of cholesterol sulfate (data not shown) were detected, indicating that other sulfotransferase(s) are responsible for its biosynthesis. Although the expression of *Cst* gene was completely eliminated in the homozygous mutant mouse, no changes in mRNA expression levels of myelin-specific proteins CGT, myelin-associated glycoprotein, myelin basic protein, and proteolipid protein were observed (Fig. 2*C*), suggesting that $Cst^{-/-}$ oligodendrocytes undergo the normal differentiation process.

Histological analysis revealed that axons were well myelinated in $Cst^{-/-}$ mice, but myelin vacuolation was observed in the cerebellar white matter, diencephalon, brainstem, and the spinal anterior column as noted in CGT-deficient mice (14), although in a lesser degree (Fig. 2*D Left*). In addition, focal axonal swelling (axonal spheroid formation) was conspicuous in the cerebellar white matter and in the granular layers (Fig. 2*D Right*), suggesting secondary neuronal degeneration caused by abnormalities in myelination (20). Electron microscopic analysis of myelinated nerve fibers revealed disorganized termination of the lateral loops at the node of Ranvier, similar to that reported in $Cgt^{-/-}$ mice (21) (Fig. 2*E*). Detailed analysis of the fine structure at the axoglial junction is not yet complete. Sulfatide may play a role in nodal formation by mediating axoglial interactions as an adhesion molecule for cell–cell interactions as reported (7). Despite the significant symptoms and morphological abnormalities observed here, maximal nerve conduction velocity of the sciatic motor nerve and the pyramidal tract fibers remained normal until 18 weeks (Fig. 2*F*). The reason for this discrepancy remains to be investigated.

$Cst^{-/-}$ males were infertile, whereas females were able to breed. The average testis weight of the $Cst^{-/-}$ mice (28.2 ± 6.8 mg; $n = 8$) was approximately 35% of that of wild-type littermates (90.2 ± 12.3 mg; $n = 8$) at 12 weeks of age (Fig. 3*A*). No sperm was observed in the epididymis of $Cst^{-/-}$ males, in contrast to wild-type or heterozygous mice (data not shown). Normal size of the seminal vesicles of CST-knockout mice indicates unaltered Leydig-cell function in the knockout mice (Fig. 3*A*). The *Cst*-null mice lacked seminolipid in the testis (Fig. 3*B*), proving that the *Cst* gene is also responsible for the biosynthesis of seminolipid *in vivo*. In contrast to the brain, the precursor GalEAG markedly accumulated in $Cst^{-/-}$ testis (Fig. 3*B*). Because seminolipid accounts for much more than GalEAG in normal adult testis (16), the blockage of the biosynthetic pathway presumably leads to an accumulation of the precursor. In addition, some change was observed in long-chain glycolipids in the $Cst^{-/-}$ testis (Fig. 3*B*), which may reflect the difference in the population of resident germ cells.

Histologically, haploid cells and secondary spermatocytes were absent from the seminiferous tubules of the $Cst^{-/-}$ mice, whereas spermatogonia and primary spermatocytes seemed normal (Fig. 3*C*). The Leydig and Sertoli cells also seemed to be normal in $Cst^{-/-}$ mice. Late spermatocytes exhibited degeneration ranging from nuclear condensation to the formation of syncytial multinucleated cells at the metaphase of the first meiotic division (Fig. 3*C*, arrows), indicating an abrupt arrest of

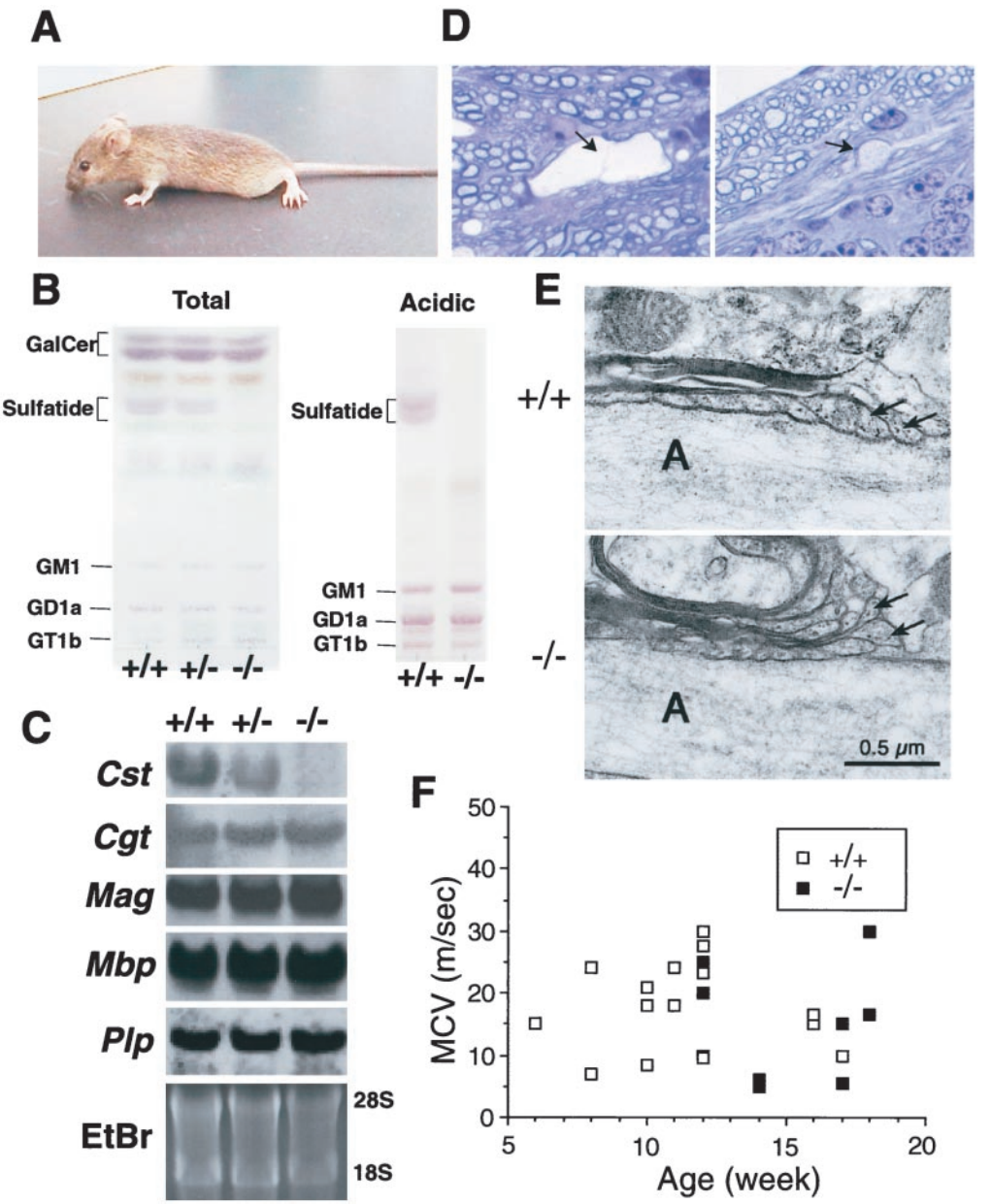

Fig. 2. Neurological abnormalities in $Cst^{-/-}$ mice. (*A*) Postural abnormality of $Cst^{-/-}$ mice. The mutant mice dragged their hindlimbs during walking and their posture was flat because of the hindlimb weakness. Knockout mice were not able to grip a horizontal bar with their forelimbs, suggesting that the forelimbs are also weak. (*B*) Glycolipid analysis of brains from 12-week-old wild-type (+/+), heterozygous (+/−), and homozygous (−/−) littermates. Total (*Left*) and acidic (*Right*) lipid fractions, corresponding to 0.5 mg of protein, were chromatographed on precoated Silica Gel 60 HPTLC plates (Merck) by using the solvent systems: chloroform/methanol/water (60:35:8 by volume) and chloroform/methanol/0.2% $CaCl_2$ (60:40:9 by volume), respectively, along with standard glycolipids. Orcinol/sulfuric acid was used for the detection of glycolipids. The positions of standard glycolipids are indicated on the left. (*C*) Northern blot analysis of myelin-marker genes. Total brain RNA from 12-week-old wild-type (+/+), heterozygous (+/−), and homozygous mutant (−/−) mice was hybridized with *Cst*, *Cgt*, *Mag*, *Mbp*, and *Plp* probes. Ethidium bromide (EtBr) staining of 28S and 18S ribosomal RNA is shown as a loading control. (*D*) Histologic analysis of cerebellum sections from a 13-week-old $Cst^{-/-}$ mouse. Myelin splitting (*Left,* arrow) and axonal spheroid body (*Right,* arrow) were observed. (*E*) Ultrastructure of the axoglial junction at a node of Ranvier of the myelinated fiber in cerebellar white matter from a 13-week-old wild-type (+/+) and homozygous mutant (−/−) mouse. In the mutant mouse, paranodal loops (arrows) were turned away from the axon (*A*). (*F*) Electrophysiological analysis of peripheral nerve conductivity. Maximal conduction velocity of sciatic motor nerve was measured on $Cst^{+/+}$ (open square) and $Cst^{-/-}$ (closed square) mice of various ages.

spermatogenesis during the late meiotic prophase in $Cst^{-/-}$ males. The terminal deoxynucleotidyltransferase-mediated dUTP-biotin nick end-labeling assay indicated that the degenerating cells were undergoing apoptosis (Fig. 3*D*).

To verify the stages of the developmental arrest of spermatogenic cells in $Cst^{-/-}$ mice, the expression of spermatogenesis-marker genes was examined by semiquantitative RT-PCR analysis (Fig. 3*E*). *Hlf3* (encoding histone H1t) is expressed in mid- to late-pachytene spermatocytes (22) and *Sprm1* is transiently expressed from late-pachytene to diprotene (23). The transcripts from these genes were present in $Cst^{-/-}$ testes at the same levels as in the wild type. The *Ccna1* (encoding cyclin A1) gene is expressed just before or during the first meiotic division (24). *Cdc25c* transcripts first appear in late pachytene-diprotene

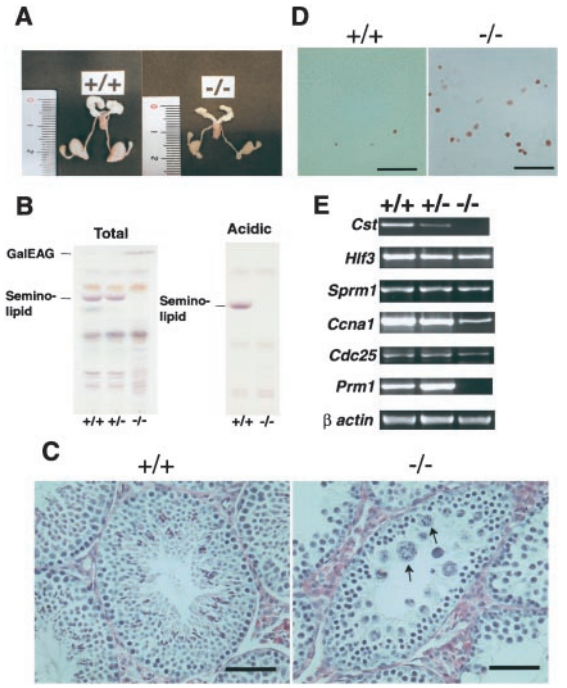

Fig. 3. Spermatogenesis abnormalities in $Cst^{-/-}$ mice. (*A*) Male genital organs from 8-week-old wild-type (+/+) and homozygous mutant (−/−) littermates. (*B*) Glycolipid analysis of testes from 8-week-old wild-type (+/+), heterozygous (+/−), and homozygous mutant (−/−) littermates. Total and acidic lipid fractions, corresponding to 2 mg of protein, were chromatographed and stained as described for Fig. 2*B*. The positions of standard glycolipids are indicated on the left. (*C*) Histologic analysis of testis sections from 8-week-old wild-type (+/+) and mutant (−/−) littermates. (Scale bars = 50 μm.) Arrows indicate the characteristic syncytial multinucleated cells. (*D*) Detection of germ cell apoptosis. *In situ* terminal deoxynucleotidyltransferase-mediated dUTP-biotin nick end-labeling staining in the seminiferous tubules of 4-week-old wild-type (+/+) and $Cst^{-/-}$ (−/−) mice. An increase of luminal distributed apoptotic cells (brown) in the tubules of mutant testis is evident; only physiological apoptotic cells of spermatogonia are seen in wild-type testes. (Scale bars = 50 μm.) (*E*) RT-PCR analysis of spermatogenesis-marker genes. Total RNA from 12-week-old wild-type (+/+), heterozygous (+/−), and homozygous (−/−) testes was used as template. β-Actin RNA is shown as a loading control.

spermatocytes and are abundant in round spermatides (25). The messages for *Ccna1* and *Cdc25c* were significantly reduced in the homozygous mutant mice as compared with wild-type and heterozygous mutant mice. $Cst^{-/-}$ testes completely lacked the haploid-specific *Prm1* transcript (encoding protamine 1) (26), indicating that spermatogenesis of the mutant mice was blocked before the meiotic division. Thus, the results of the gene-expression experiments are consistent with the morphological observations in that the spermatogenesis of $Cst^{-/-}$ mice is arrested at the end of the meiotic prophase. The arrested stage in $Cst^{-/-}$ mice seems to be somewhat later than that in $Cgt^{-/-}$ mice, in which the metaphase of meiosis was not observed and the expression of late-pachytene spermatocyte-marker genes *Hlf3* and *Sprm-1* was reduced (16). These findings suggest that GalEAG and seminolipid are successively involved in the genetic program of spermatogenesis in the same order as their biosynthesis. Because these glycolipids are expressed on the cell surface of primary spermatocytes from the end of the leptotene stage or the zygotene stage and later (7, 8, 16), the interaction between Sertoli cells and spermatocytes, which is known to be important for their differentiation (27), may be disrupted in these knockout mice.

GalCer and sulfatide together constitute approximately 30% of total myelin lipid, and they are first expressed at a critical point during oligodendrocyte differentiation, when progenitors cease to proliferate and commence terminal differentiation. This fact leads to the prediction that these lipids play a role in the regulation of oligodendrocyte differentiation, in addition to their eventual roles as structural components of mature myelin. Indeed, oligodendrocyte differentiation is enhanced in CGT-knockout mice *in vitro* and *in vivo*, indicating that GalCer and/or sulfatide act as negative regulators of the entry of oligodendrocytes into terminal differentiation (28). Furthermore, the terminal differentiation was blocked by anti-sulfatide antibody O4 but not by anti-GalCer antibody O1 (28). These findings strongly suggest that sulfatide is a key regulator of the oligodendrocyte differentiation. This hypothesis must be certified by using CST-knockout mice.

The observed differences in phenotype between CGT- and CST-deficient mice revealed that GalCer and GalEAG act, not only as a precursor for sulfoglycolipid synthesis, but also as a functional molecule in myelin function and spermatogenesis, respectively. It also indicates that sulfate group-recognizing mechanisms are involved in such biological processes. By comparing the differences between CGT- and CST-deficient mice in detail, a differentiation in the molecular mechanisms in which the galactolipids and sulfoglycolipids are involved could be drawn. The quantitatively minor sulfated glycolipids include lactosylceramide sulfate and SM1b, which are found in the kidney and small intestine, respectively (7). Their sulfation is catalyzed by CST *in vitro* (10), whereas CGT is not involved in the biosynthetic pathway of these glycolipids. Therefore, a phenotype specific to CST-deficient mice had been expected. However, $Cst^{-/-}$ mice exhibited signs of neither renal failure nor digestive disorders, and they were able to survive for more than 1 year. No apparent histologic abnormality was noticed in the kidney and alimentary system. A detailed analysis is needed to elucidate the biological function of sulfated glycolipids in the kidney and alimentary canal. The significance of monogalactosyldiacylglycerol sulfate, which is present as a minor component in the brain of very young mice as well as in the testis (7), also remains to be investigated.

Because *Cst*-null mice are not embryonic lethal, a human disease with inherited CST deficiency may exist. Thus far, no such human neuropathological diseases have been mapped in the vicinity of the *CST* locus on chromosome 22q12 (13). The CST-knockout mouse may provide a symptomatic model for a search for a human CST deficiency.

We thank Ms. T. Usami and Ms. R. Okamoto for their help in injecting embryonic stem cells into blastocysts, Dr. Y. Nishimune for critical comments on the histologic observation of testis, and Dr. M. Taniike for help in tissue preparation for the morphological study of the nervous system. We are also grateful to Dr. K. Suzuki for his critical reading of this manuscript. This work was supported by grants from the Naito Foundation and the Ministry of Education, Culture, Sports, Science and Technology of Japan (Priority Area 1078104) to K.H. and by Research Grants NS 27736 (to B.P.) and NS 24453 (to K.S.), and Mental Retardation Research Center Core Grant HD 03110 from the U.S. Public Health Service.

1. Bullock, S. L., Fletcher, J. M., Beddington, R. S. P. & Wilson, V. A. (1998) *Genes Dev.* **12,** 1894–1906.
2. Humphries, D. E., Wong, G. W., Friend, D. S., Gurish, M. F., Qiu, W. T., Huang, C., Sharpe, A. H. & Stevens, R. L. (1999) *Nature (London)* **400,** 769–772.
3. Forsberg, E., Pejler, G., Ringvall, M., Lunderius, C., Tomasini-Johansson, B., Kusche-Gullberg, M., Eriksson, I., Ledin, J., Hellman, L. & Kjellen, L. (1999) *Nature (London)* **400,** 773–775.
4. Tangemann, K., Bistrup, A., Hemmerich, S. & Rosen, S. D. (1999) *J. Exp. Med.* **190,** 935–942.

5. Akama, T. O., Nishida, K., Nakayama, J., Watanabe, H., Ozaki, K., Nakamura, T., Dota, A., Kawasaki, S., Inoue, Y., Maeda, N., *et al.* (2000) *Nat. Genet.* **26,** 237–241.
6. Hemmerich, S., Bistrup, A., Singer, M. S., van Zante, A., Lee, J. K., Tsay, D., Peters, M., Carminati, J. L., Brennan, T. J., Carver-Moore, K., *et al.* (2001) *Immunity* **15,** 237–247.
7. Ishizuka, I. (1997) *Prog. Lipid Res.* **36,** 245–319.
8. Vos, J. P., Lopes-Cardozo, M. & Gadella, B. M. (1994) *Biochim. Biophys. Acta* **1211,** 125–149.
9. Pfeiffer, S. E. Warrington, A. G. & Bansal, R. (1993) *Trends Cell Biol.* **3,** 191–197.
10. Honke, K., Yamane, M., Ishii, A., Kobayashi, T. & Makita, A. (1996) *J. Biochem.* **119,** 421–427.
11. Honke, K., Tsuda, M., Hirahara, Y., Ishii, A., Makita, A. & Wada, Y. (1997) *J. Biol. Chem.* **272,** 4864–4868.
12. Hirahara, Y., Tsuda, M., Wada, Y. & Honke, K. (2000) *Eur. J. Biochem.* **267,** 1909–1916.
13. Tsuda, M., Egashira, M., Niikawa, N., Wada, Y. & Honke, K. (2000) *Eur. J. Biochem.* **267,** 2672–2679.
14. Coetzee, T., Fujita, N., Dupree, J., Shi, R., Blight, A., Suzuki, K., Suzuki, K. & Popko, B. (1996) *Cell* **86,** 209–219.
15. Bosio, A., Binczek, E. & Stoffel, W. (1996) *Proc. Natl. Acad. Sci. USA* **93,** 13280–13285.
16. Fujimoto, H., Tadano-Aritomi, K., Tokumasu, A., Ito, K., Hikita, T., Suzuki, K. & Ishizuka, I. (2000) *J. Biol. Chem.* **275,** 22623–22626.
17. Tohyama, J., Vanier, M. T., Suzuki, K., Ezoe, T., Matsuda, J. & Suzuki, K. (2000) *Hum. Mol. Genet.* **9,** 1699–1707.
18. Committee on Care and Use of Laboratory Animals (1985) *Guide for the Care and Use of Laboratory Animals* (Natl. Inst. Health, Bethesda), DHHS Publ. No. (NIH) 85–23.
19. Kakuta, Y., Pedersen, L. G., Carter, C. W., Negishi, M. & Pedersen, L. C. (1997) *Nat. Struct. Biol.* **4,** 904–908.
20. Suzuki, K. & Zagoren, J. C. (1975) *Brain Res.* **85,** 38–43.
21. Dupree, J. L., Coetzee, T., Blight, A., Suzuki, K. & Popko, B. (1998) *J. Neurosci.* **18,** 1642–1649.
22. Kremer, E. J. & Kistler, W. S. (1991) *Exp. Cell Res.* **197,** 330–332.
23. Andersen, B., Pearse, R. V., II, Schlegel, P. N., Cichon, Z., Schonemann, M. D., Bardin, C. W. & Rosenfeld, M. G. (1993) *Proc. Natl. Acad. Sci. USA* **90,** 11084–11088.
24. Ravnik, S. E. & Wolgemuth, D. J. (1999) *Dev. Biol.* **207,** 408–418.
25. Wu, S. & Wolgemuth, D. J. (1995) *Dev. Biol.* **170,** 195–206.
26. Kleene, K. C., Distel, R. J. & Hecht, N. B. (1984) *Dev. Biol.* **105,** 71–79.
27. Jegou, B. (1993) *Int. Rev. Cytol.* **147,** 25–96.
28. Bansal, R., Winkler, S. & Bheddah, S. (1999) *J. Neurosci.* **19,** 7913–7924.